Active damping with piezoelectric MEMS devices

M. Collet[a], V. Walter[a], P. Delobelle[a]

[a]FEMTO-ST, LMA R. Chaléat, UMR 6174, 25000 Besancon, France

ABSTRACT

Thick PZT films are of major interest in the actuation of mechanical structures. One of the promising fields deals with active damping. Piezoelectric actuators have proved to be effective control devices for active stabilization of structural vibrations and are now used in a wide range of engineering applications. Piezo materials can be integrated in various structural components as distributed sensors or actuators. In this context, Micro-Electro-Mechanical Systems appear very attractive in improving the mechanical efficiency of structural active control. These systems can be distributed on a structure and are very powerful since it induces a very high level of stress density. They can effectively present a good opportunity in a large class of problem. The studied micro controlling system is a micro beam totally covered by a piezoelectric, PZT, film. This sample system can be considered as a suspension element being able to support very light and sensitive systems like frequency generator or MEMS sensors. We first describe modeling and the experimental updating methods used to characterize piezoelectric behavior. Secondly, we show the observations highlighting the efficiency of hard-PZT thick films in active damping of sensitive devices by using pseudo direct velocity feedback.

Keywords: Piezelectric thin layers, MEMS transducers, Sky-hook active isolation

1. INTRODUCTION

Piezoelectric actuators have proved to be effective control devices for active control of structural vibrations and are now used in a wide range of engineering applications. Piezo materials are widely use in active control of vibrating structures as well as sensors as actuators. The books of Preumont[1] and Banks[2] present a large overview of these material applications. The induced electro-mechanical coupling and the partial derivative equations driving the behavior of such a material is found in Banks,[2] Lee,[3] ,[4] ,[5] Kim[6] or Tzou.[7]

Many works on structural active control as in Tzou,[8] Gaudenzi,[9] Preumont[1] or Lara and Sloss,[10,11] shows that the only stable, robust and efficient class of strategy implemented in a mechanical structure is the collocated active damping feedback strategies. Even if some works aim at optimizing uncollocated transducers setup like in Collet,[12] Lee,[5] Hac[14] and even if it is known that the boundary uncollocated approach is much more efficient (see Bourquin[15] or Komornik[16]), it seems difficult today to use uncollocated strategy while guaranteeing some good robustness properties.

In this context, Micro Electro Mechanical Systems seem to be very interesting to improve the mechanical efficiency of structural active control. Indeed, these systems can be distributed, quasi collocated, on a structure. They can effectively present a good opportunity in a large class of problems : waves control like in Carva,[17] control of the mechanical interaction or the stabilization of a microsystem like those described in Yee.[18]

We have first studied the control of a micro beam totally covered by a piezoelectric, PZT, film. This sample system can be considered as a suspension element being able to support very light and sensitive systems like a frequency generator. The obtained mechanical properties of this micro controlling system is also studied in terms of mechanical characterization of the hard-PZT screen-printed films like in Seffner[19] and of experimental analysis of the properties of the proposed control system.

2. THEORITICAL MODELING

The studied mechanical system is shown in Figure 1. It deals with an alumina cantilever beam on which a PZT film is screen-printed.[19] The constitutive layers of the cantilever beams are also shown in Figure 1.

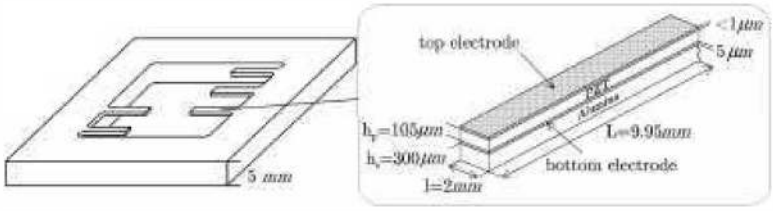

Figure 1. Geometry of the mechanical system.

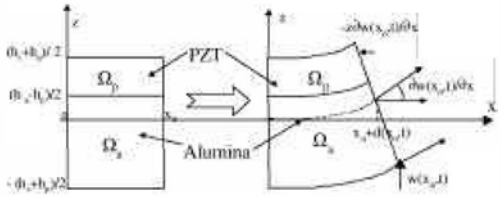

Figure 2. Kinematical assumptions of Kirchoff Love homogenization technique.

2.1. Constitutive relations of the laminated piezocomposite

The piezoelectric layer is assumed to be polarized along (Oz) and all materials are assumed to be isotropic or isotropic in the plane (Oxz). Consider the bending motion in plane $(0xz)$ of an Euler-Bernoulli beam (figure 2) the piezoelectric state equation can be restricted in equations (1) as in Banks[2] or Lee[5] :

$$\begin{aligned} \sigma_{xx}(x,z,t) &= E_p \varepsilon_{xx}(x,z,t) - e_{31}E \qquad \forall (x,z) \in \Omega_p, \\ D_z &= e_{31}\varepsilon_{xx}(x,z,t) + \epsilon.E \qquad \forall (x,z) \in \Omega_p, \end{aligned} \tag{1}$$

where σ_{xx} is the (xx) component of the stress tensor, ε_{xx} is the corresponding strain, the Young's modulus of the piezoelectric layer E_p is assumed to be independent of the thickness, e_{31} is the piezoelectric constant, E is the electric field, D_z the electric displacement along the polarization axis (Oz) and ϵ is the dielectric permittivity. The first equation reflects the reverse piezoelectric coupling effect and the second expresses the direct one. We introduce the electric potential V by assuming the linear variation of E along the thickness negligible in comparison with the constant part : $V = -E.h_p$. Similarly, the constitutive relation for the alumina layer is given by equation (2) :

$$\sigma_{xx}(x,z,t) = E_s \varepsilon_{xx}(x,z,t) \qquad \forall (x,z) \in \Omega_s. \tag{2}$$

The bending displacement of the cross section of the considered Euler-Bernoulli beam is described in Figure 2. The cross section displacement is given by : $d(x,z,t) = d(x,t) - z\frac{\partial w(x,t)}{\partial x}$ where $d(x,t)$ is the displacement along (Ox) at $z = 0$, and $w(x,t)$ is the transverse displacement of the section along (Oz). All these assumptions lead us to a Kirchoff-Love homogenization of the motion in the lamina. The expressions of the in-plane normal force and the bending moment along (Oy) applied on each cross section give us the classical constitutive relations of the composites :

$$\begin{aligned} N(x,t) &= A_{11}\frac{\partial d(x,t)}{\partial x} + B_{11}(-\frac{\partial^2 w(x,t)}{\partial x^2}) + l e_{31} V(t), \\ M(x,t) &= B_{11}\frac{\partial d(x,t)}{\partial x} + D_{11}(-\frac{\partial^2 w(x,t)}{\partial x^2}) + \tfrac{h_s}{2} l e_{31} V(t), \end{aligned} \tag{3}$$

where the homogenized stiffness coefficients are given by :

$$\begin{aligned} A_{11} &= (E_s h_s + E_p h_p) l, \\ B_{11} &= \tfrac{E_p - E_s}{2} h_p h_s l, \\ D_{11} &= \frac{E_s h_s (h_s^2 + 3h_p^2) + E_p h_p (h_p^2 + 3h_s^2)}{12} l. \end{aligned} \tag{4}$$

Equations (3) show that the in-plane and bending motions are coupled through the term B_{11}. The dynamical equilibrium of the composite Euler-Bernoulli beam is driven by the global equation of our system expressed in (5).

$$\begin{aligned}
&\bar{\rho}\frac{\partial^2 d(x,t)}{\partial t^2} - A_{11}\frac{\partial^2 d(x,t)}{\partial x^2} + B_{11}.\frac{\partial^3 w(x,t)}{\partial x^3} = 0 \qquad \forall x \in]0, L[,\\
&\bar{\rho}\frac{\partial^2 w(x,t)}{\partial t^2} - B_{11}\frac{\partial^3 d(x,t)}{\partial x^3} + D_{11}.\frac{\partial^4 w(x,t)}{\partial x^4} = 0 \qquad \forall x \in]0, L[,\\
&+\text{Initial Conditions.}
\end{aligned} \tag{5}$$

The boundary conditions are given in equations (6) :

$$\begin{aligned}
w(0,t) = d(0,t) = \frac{\partial w(0,t)}{\partial x} = 0,\\
A_{11}\frac{\partial d(L,t)}{\partial x} - B_{11}.\frac{\partial^2 w(L,t)}{\partial x^2} = -l.e_{31}.V(t),\\
-B_{11}\frac{\partial d(L,t)}{\partial x} + D_{11}.\frac{\partial^2 w(L,t)}{\partial x^2} = \frac{h_s}{2}.l.e_{31}.V(t),\\
-B_{11}\frac{\partial^2 d(L,t)}{\partial x^2} + D_{11}.\frac{\partial^3 w(L,t)}{\partial x^3} = 0.
\end{aligned} \tag{6}$$

In the following developments, the kinetic energy associated to the term $\bar{\rho}\frac{\partial^2 d(x,t)}{\partial t^2}$ in the in-plane motion equation (5) is assumed to be negligible. So, the corresponding constitutive equation (the first one in (5)) can be simplified so as : $\frac{\partial^2 d(x,t)}{\partial x^2} = \frac{B_{11}}{A_{11}}\frac{\partial^3 w(x,t)}{\partial x^3} \qquad \forall x \in]0, L[$. The first equation (5) is thus condensed in the sense of Guyan. The new system of equations governing the motion of our system is also written in equation (7) :

$$\begin{aligned}
&\bar{\rho}\frac{\partial^2 w(x,t)}{\partial t^2} + E_{co}I_{co}.\frac{\partial^4 w(x,t)}{\partial x^4} = 0 \qquad \forall x \in]0, L[,\\
&+\text{Initial Conditions},
\end{aligned} \tag{7}$$

where $E_{co}I_{co} = (D_{11} - \frac{B_{11}^2}{A_{11}})$. The associated boundary equations are given in (8) :

$$\begin{aligned}
w(0,t) = \frac{\partial w(0,t)}{\partial x} = 0\\
E_{co}I_{co}.\frac{\partial^2 w(L,t)}{\partial x^2} = G_p.V(t)\\
\frac{\partial^3 w(L,t)}{\partial x^3} = 0,
\end{aligned} \tag{8}$$

where $G_p = (\frac{h_s}{2} - \frac{B_{11}}{A_{11}})le_{31}$ and $e_{31} = d_{31}E_p$.

Thus, we obtain the classical set of equations for a bent beam with a modified stiffness. The force induced by the voltage is the pure bending torque applied at the boundary limit of the piezoceramic layer ($x = L$) like in Banks,[2] Lee[5] and Collet.[12]

3. EXPERIMENTAL INVESTIGATIONS

3.1. Fabrication of the samples

The mechanical system (Figure 1) is a rack of alumina cantilever beams on which a PZT film is screen-printed (see Seffner[19]). The alumina beams are thus clamped at one end to a stiff frame so that good clamping conditions

are guaranteed. The constitutive layers of the cantilever beams are also shown in Figure 1. The first layer is an Ag-Pd bottom electrode screen-printed on the alumina substrate. The second layer consists of the active material, the hard-PZT material. This active layer is also screen-printed using a paste containing a powder of $PbSr\,(Zr_{0.455}Ti_{0.455}W_{0.036}Sn_{0.036}Mn_{0.028})$, fabricated by the Ferroelectricity and Electrical Engineering Laboratory (Lyon, France) (see Tajan[21]). The top layer is a sputtered gold electrode. Once the fabrication process is finished, it is necessary to pole the film so that it will exhibit better dielectric, ferroelectric and piezoelectric properties. It is known that the deposition process always induces a loss of properties compared to the bulk material. As a consequence, an electromechanical characterization is worth to determine the elastic modulus E_p and the piezoelectric coefficient d_{31} (or $e_{31} = E_p d_{31}$) of the film.

3.2. Electromechanical characterization

3.2.1. Mechanical tests

The mechanical experiments involve a dynamic bending test, a quasi-static bending test and a nanoindentation test. Both bending tests end up with an experimental parameter X that will allow the computation of the elastic modulus. The Young's modulus is indeed the positive solution of the second order polynomial given by :

$$AE_p^2 + BE_p + C = 0, \tag{9}$$

with :

$$\begin{aligned} A &= h_p^4, \\ B &= 2E_s h_s h_p \left(2h_s^2 + 2h_p^2 + 3h_s h_p\right) - h_p X, \\ C &= E_s^2 h_s^4 - E_s h_s X \end{aligned} \tag{10}$$

where the parameters E_i and h_i are respectively the elastic modulus and the thickness. The subscripts $i = s$ and $i = p$ refer to the substrate and the piezoelectric film. For the dynamic test, the parameter X is equal to :

$$X_{dyn} = \frac{48\pi^2 L^4 \left(h_p \rho_p + h_s \rho_s\right)}{p_i^4} \left(f_i\right)_{\exp}^2, \tag{11}$$

where L is the length of the beam, ρ_p and ρ_s are respectively the mass density of the piezoelectric film and the substrate, f_i and p_i are respectively the experimental eigenfrequency and the frequency parameter of the i^{th} mode. Note that the porosity of the piezoelectric film is taken into account in the value of ρ_p.

For the quasi-static test, the value of X is given by :

$$X_{sta} = \frac{4L^3}{l} \left(\frac{F}{\delta}\right)_{\exp}, \tag{12}$$

where F is the applied load, δ the corresponding deflection and l is the width of the beam.

In the case of the nanoindentation test, the value of the elastic modulus is expressed in :

$$\frac{E}{1-\nu^2} = \left(\frac{2\sqrt{A}}{\sqrt{\pi}} \left(\frac{dh}{dP}\right)_{\exp} - \frac{1-\nu_i^2}{E_i}\right)^{-1}, \tag{13}$$

where ν is the Poisson's ratio of the tested material (assuming to be equal to 0.3), A is the projected contact area, $\left(\frac{dP}{dh}\right)_{\exp}$ is the experimental contact stiffness and E_i and ν_i are respectively the Young's modulus and Poisson's ratio for diamond.[23]

Table 1 summarizes the results derived from the different tests. In this Table, $N_{measure}$ represents the number of measures performed for both types of materials, the substrate and the piezoelectric film. It can be seen that the results are homogeneous from one test to another. In the case of alumina, the difference between the calculated

Table 1. Elastic modulus of alumina and hard-PZT calculated from the different mechanical tests

	Al_2O_3	Hard-PZT
$N_{measure}$	15	22
$E_{dynamic}$	$335 \pm 5GPa$	$19 \pm 6GPa$
$N_{measure}$	71	19
E_{static}	$340 \pm 8GPa$	$21 \pm 8GPa$
$N_{measure}$	20	30
E_{nano}	$341 \pm 45GPa$	$29 \pm 4GPa$
E_{bulk}	$350GPa$	$94GPa$

value and the value of the bulk is roughly around $10GPa$, which is less than 3% of the bulk. For the hard-PZT, the values calculated from the different tests are much lower than the value of the bulk material. It is thought to be related to the porosity of the film. In this case, the porosity represents indeed near 50% of the total volume of the film, which causes a serious drop in elastic properties.

3.2.2. Electromechanical tests

Once the mechanical properties of the films are determined, we can study the influence of the deposition process on the piezoelectric coefficient d_{31}. This coefficient relates the strain in the x direction when the film is subjected to a voltage in the perpendicular z direction. For a piezocomposite cantilever beam, one can derive the expression of d_{31} from static version of equation (7):

$$d_{31} = -\frac{4E_{co}I_{co}\left(E_s h_s + E_p h_p\right)}{E_s E_p h_s \left(h_s + h_f\right).l.L^2} \cdot \frac{\delta}{V}, \tag{14}$$

where V is the applied voltage, δ is the corresponding displacement at the free end of the beam and :

$$E_{co}I_{co} = \left(\frac{E_s^2 h_s^4 + 2E_s E_p h_s h_p \left(2h_p^2 + 3h_p h_s + 2h_s^2\right) + E_p^2 h_p^4}{12\left(E_p h_p + E_s h_s\right)}\right) l. \tag{15}$$

These expressions are deduced from the theoretical modeling developed in the first section. Two testing benches were set up : one uses the nanoindenter to measure the deflection at the tip of the beam and the other one uses an optical probe. Using these experiments, an average value of the piezoelectric coefficient d_{31} was found :

$$d_{31} = -25 \pm 3pC/N \tag{16}$$

Once again, this value is much lower than the value of the bulk, idest $-108pC/N$. The porosity of the films seems to be a nice explanation for the drop of the electromechanical properties as previously mentioned.

The alumina and piezoelectric layers have also respectively the mechanical characteristics given in Table 2.

3.3. Experimental setup for active control tests

The aim of our investigations is to show the capability of this system to induce high damping effect through the control of the piezoceramic layer. For this purpose the micro-beam is introduced in a feedback loop as described in Figure 3. The active beam is clamped to a rigid frame of alumina. The piezoelectric plate glued on the frame is used as an external excitator (Figure 3). A laser vibrometer measures the velocity of the beam at $x = L$ in the mid-width. The output signal of the vibrometer is also amplified and directly applied as a controlling signal on the piezoceramic layer of the beam. In the meantime, a measurement system Siglab© produces the excitation signal applied to the external piezoelectric plate and measures the output signal of the vibrometer in order to compute the related transfer functions.

Table 2. Mechanical characteristics of the alumina and piezoelectric layers

	alumina	piezoelectric
Length	$9.95mm$	$9.95mm$
Width	$2mm$	$2mm$
Thickness	$300\mu m$	$110\mu m$
Young Modulus	$340GPa$	$22GPa$
Mass Density	$3900kg.m^{-3}$	$4000kg.m^{-3}$(0.5 bulk)
Piezoelectric coefficient (e_{31})	0	$-0.55N.m^{-1}V^{-1}$

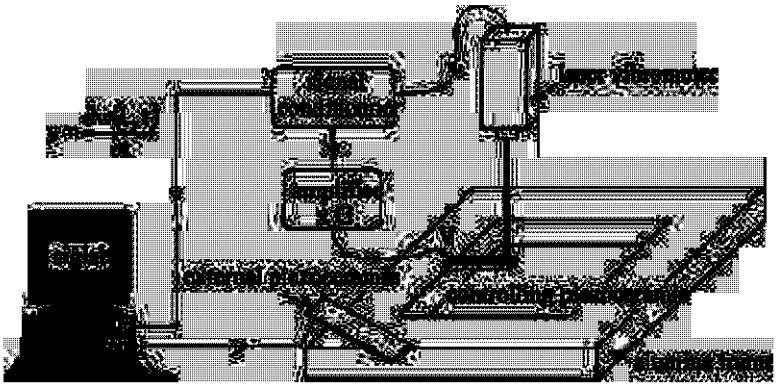

Figure 3. Experimental setup : mechanical system and control feedback loop.

3.4. Experimental results

The Frequency Response Functions of the system are computed for different levels of the gain G. Figure 4 presents two Frequency Response Functions. The dot-line curve represents the response before the control is applied and the solid-line curve corresponds to the maximum value of the gain G.

It can be seen from these curves that the attenuation can reach up to $43dB$. The first eigenmode of the beam is completely damped for this value which means that the critical damping is reached. It is also to notice that the second resonance peak at $7.5kHz$ is due to a mode involving the alumina frame so that it is not affected by the control. We underline here that no instability occurs during the test. The maximum gain G is just limited by the power of the voltage amplifier used in the control loop. This experiment seems to show that instability does not appear for this uncollocated system.

The mechanical system modeled in the previous section is controlled according to the strategy presented on Figure 3. The applied voltage $V(t)$ in equation (8) is proportional to the output signal corresponding to the transverse velocity in the form $V(t) = -g\frac{\partial w(L,t)}{\partial t}$. So, the boundary control strategy implemented onto the beam appears to be a pseudo direct velocity feedback that can be compared with Direct Velocity Feedback described in Preumont.[1] The applied controlling force and the measured signal are indeed collocated but in our case they do not correspond to dual quantities. A true direct velocity feedback (DVF) would lead to apply a controlling voltage given by $V(t) = -g\frac{\partial^2 w(L,t)}{\partial t \partial x}$ in order to impose dual dissipative term when $g > 0$ as it is shown in Preumont.[1] We have proved in Collet and al[13] that this quasi-collocated control strategy is unconditionally stable for any feedback gain G.

4. CONCLUDING REMARKS

The experiment presented in this paper shows the real efficiency of the hard-PZT thick films in actuating microstructures. It is observed that the typical attenuation can reach up to $43db$ on the first mode before being critical without inducing spill-over instability. While our structure is not strictly collocated, this result appears very

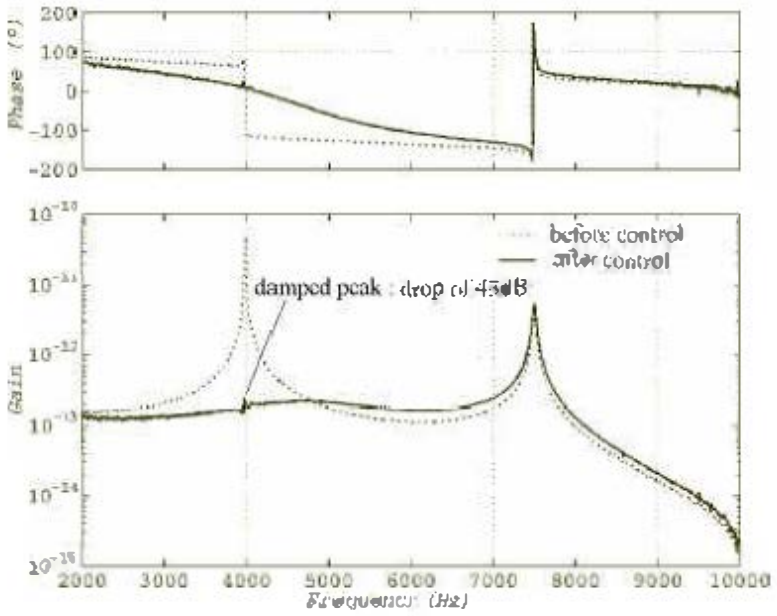

Figure 4. Frequency Response Function of a piezocomposite beam before and after control.

surprising according to Preumont[1] or collet.[2] Thus the classical property of conditional instability of the non collocated controlled systems may be refuted .

This result underlines the necessity to use some specific techniques to study the controlled behavior of a continuous structure as reported by[15,16] or.[10] Applying directly automation tools on a finite element modeling of the mechanical system can lead to numerical misunderstanding as described in Collet and al.[13] As we use more and more efficient actuators in the systems, it really appears essential to develop new numerical tools dedicated to design structural boundary control strategy especially for Micro Electro Mechanical System applications.

REFERENCES

1. A. Preumont, *Vibration control of active structures, an introduction*. Dordrecht/Boston/London: Kluwer Academic Publishers, 1997.
2. H.T. Banks, R.C. Smith, *Smart Material Structures Modeling Estimation and Control*, Paris: J. Wiley Sons and Masson Publishers, 1996
3. C.K Lee, *Laminated piezopolymer plates for torsion and bending sensors and actuators*. Journal of Acoustical Society of America, 85(6), 2432-2439. , 1989.
4. C.K Lee, *Theory of laminated piezoelectric plates for design of distributed sensors/actuators. Part I : Governing equations and reciprocal relationships*, Journal of Acoustical Society of America, 87(3), 1144-1158, 1990.
5. C.K Lee, W-W Chiang, T.C O'Sullivan, *Piezoelectric modal sensor/actuator pairs for critical active damping vibration control*, Journal of Acoustical Society of America, 90(1), 374-384, 1991.
6. U. Lee, J. Kim, *Spectral element modeling for the beams treated with active constrained layer damping*, International Journal of Solids and Structures, 38, 5679-5702, 2001
7. H.S. Tzou, H.Q. Fu, *A study of segmentation of distributed piezoelectric sensors and actuators. Part I : Theoritical Analysis*. Journal of Sound and Vibration, 172(2), 247-259, 1994.
8. H.S Tzou, H.Q Fu, *A study of segmentation of distributed piezoelectric sensors and actuators, Part II : Parametric study and active vibration controls*, Journal of Sound and Vibration, 172(2), 261-275, 1994.

9. P. Gaudenzi, R. Carbonaro and E. Benzi, *Control of Beam vibrations by means of piezoelectric devices : theory and experiments*, Journal of Composite Structures, 50, 376-379, 2000.
10. A. Lara, J.C. Bruch Jr, *Vibration damping in beams via piezo actuation using optimal boundary control*, International Journal of Solids and Structures, 337, 6537-6554, 2000.
11. J.M. Sloss, J.C. Bruch Jr, *Piezoelectric patch control using an integral equation approach*, Thin-Walled Structures, 39, 45-63, 2001.
12. M. Collet, *Active control with piezoelectric layers optimization*, Journal of Structural Control,1, 59-79, 1995.
13. M. Collet, V. Walter, P. Delobelle, *Active Damping of a micro-cantilever piezo-composite beam*, Journal of Sound and Vibration, 260/3, 453 - 476, 2003.
14. A. Hac, L. Liu, *Sensor and actuator location in motion control of flexible structures*, Journal of Sound and Vibration, 167(2), 239-261, 1993.
15. F. Bourquin, M. Collet, *Some modelling and numerical issue for the control of flexible structure and their practical impact*, 3^{rd} International Workshop on Structural Control,(LCPC editor) Paris, 2000.
16. F. Bourquin, M. Collet, J.F Briffaud, *On the feedback stabilization : Komornik's methods*, 2^{nd} International Conference on Active Control in Mechanical Engineering, 1987-1997, New-York: Wiley Sons, 1997.
17. M.O.M Carvalho, M. Zindeluk, *Active control of waves in a Timoshenko beam*, International Journal of Solids and Structures, 38, 1749-1764, 2001.
18. Y. Yee, H.J Nam, *PZT actuated micromirror for fine-tracking mechanism of high-density optical data storage*, Sensors and Actuators: A Physical, 89, 199-173, 2001
19. L. Seffner and H.J. Gesemann, *Preparation and application of PZT thick films*, 4^{th} Int. Conf. on Elec. Ceramics and Appl., Electroceramics, IV 1, 317-320, 1994.
20. A. Tylikowski, *Effects of piezoactuator delamination on the transfer functions of vibration control systems*, International Journal of Solids and Structures, 38, 2189-2202, 2001.
21. V. Tajan, P. Gonnard, M. Troccazin *Elaboration of PZT thick films by screen-printing*, Proceedings of Conference on Intelligent Materials, SPIE Proc, 2779 , 564-569, 1996.
22. K. Bathe, *Finite element procedures in engineering analysis*, New-Jersey Prentice-Hall Inc.Publishers, 1982.
23. W.C Oliver, GM Pharr, *An improved Technique for determining hardness and elastic modulus using load and displacement sensing indentation experiments*, Journal of Materials Research, 7(6), 1564-1583, 1992.
24. M. Geradin, *Mechanical vibrations. Theory and application to structural dynamics*. Paris: J. Wiley Sons and Masson Publishers, 1994.
25. F. Tisseur, K. Meerbergen, *The Quadratic Eigenvalue Problem*, SIAM Review, 43(2), 235-286, 2001.